doi:10.1016/j.jmb.2006.08.017 J. Mol. Biol. (2006) 362, 1120–1131

JMB

Available online at www.sciencedirect.com

ScienceDirect

ELSEVIER

Subcellular Localization of Interacting Proteins by Bimolecular Fluorescence Complementation *in Planta*

Vitaly Citovsky[1]†, Lan-Ying Lee[2]†, Shachi Vyas[3], Efrat Glick[4] Min-Huei Chen[1], Alexander Vainstein[5], Yedidya Gafni[4] Stanton B. Gelvin[2]* and Tzvi Tzfira[3]*

[1]*Department of Biochemistry and Cell Biology, State University of New York Stony Brook, NY 11794-5215 USA*

[2]*Department of Biological Sciences, Purdue University 915 W. State Street West Lafayette, IN 47907-1392 USA*

[3]*Department of Molecular Cellular and Developmental Biology, University of Michigan, Ann Arbor MI 48109-1048, USA*

[4]*Institute of Plant Sciences A.R.O., The Volcani Center Bet Dagan 50250, Israel*

[5]*The Robert H. Smith Institute of Plant Sciences and Genetics in Agriculture, Faculty of Agricultural, Food and Environmental Quality Sciences, The Hebrew University of Jerusalem Rehovot 76100, Israel*

**Corresponding authors*

Bimolecular fluorescence complementation (BiFC) represents one of the most advanced and powerful tools for studying and visualizing protein–protein interactions in living cells. In this method, putative interacting protein partners are fused to complementary non-fluorescent fragments of an autofluorescent protein, such as the yellow spectral variant of the green fluorescent protein. Interaction of the test proteins may result in reconstruction of fluorescence if the two portions of yellow spectral variant of the green fluorescent protein are brought together in such a way that they can fold properly. BiFC provides an assay for detection of protein–protein interactions, and for the subcellular localization of the interacting protein partners. To facilitate the application of BiFC to plant research, we designed a series of vectors for easy construction of N-terminal and C-terminal fusions of the target protein to the yellow spectral variant of the green fluorescent protein fragments. These vectors carry constitutive expression cassettes with an expanded multi-cloning site. In addition, these vectors facilitate the assembly of BiFC expression cassettes into *Agrobacterium* multi-gene expression binary plasmids for co-expression of interacting partners and additional autofluorescent proteins that may serve as internal transformation controls and markers of subcellular compartments. We demonstrate the utility of these vectors for the analysis of specific protein–protein interactions in various cellular compartments, including the nucleus, plasmodesmata, and chloroplasts of different plant species and cell types.

Keywords: protein–protein interactions; plasmids; BiFC; cellular localization; YFP

† V. C. and L.-Y. L. contributed equally to this work.

Abbreviations used: BiFC, bimolecular fluorescence complementation; EYFP, YFP variant derived from EGFP; nEYFP, N-terminal part of EYFP; cEYFP, C-terminal part of EYFP; YFP, yellow spectral variant; nYFP, N-terminal YFP; cYFP, C-terminal YFP; GFP, green fluorescent protein; ECFP, enhanced cyan variant of GFP; EGFP, enhanced GFP; MCS, multi-cloning site; MP, movement protein; pSATN, modular satellite plasmids; CaMV, cauliflower mosaic virus; ORF, open reading frame; NLS, nuclear localization signal; CRT, calreticulin; ChrD, cucumber chromoplast D protein; TYLCV, tomato yellow leaf curl virus; DIC, differential interference contrast; CP, capsid protein.

E-mail addresses of the corresponding authors: gelvin@bilbo.bio.purdue.edu; ttzfira@umich.edu

Introduction

Protein–protein interactions are basic cellular events inherent to virtually every physiological process and occur in all subcellular compartments and organelles. For example, protein–protein interactions are involved in the assembly of the nuclear pore complex,[1] DNA packaging,[2] regulation of gene expression,[3] host–pathogen interactions,[4] and signal transduction.[5] The identification of interacting protein partners often provides decisive clues to unraveling the biological functions of proteins.[6] Thus, identification and characterization of specific protein–protein interactions are essential for understanding and studying various aspects of cell biology.

Various technologies have been developed for the identification and analysis of protein–protein interactions *in vitro* and *in vivo*, each with its advantages and limitations. For example, the most widely used method for *in vitro* analysis of protein–protein interactions, co-immunoprecipitation,[7] often requires the production of specific antibodies against each of the analyzed proteins, an expensive and time-consuming process. Co-immunoprecipitation also requires lysis of the cells, which generally prevents determination of the exact subcellular localization of the interacting proteins.[8,9] *In vivo* protein cross-linking and co-fractionation (including TAP tagging)[7] permit identification of protein–protein interactions, but such methods may be difficult to implement, as they involve complex biochemical procedures.

Genetic methods, such as the yeast two-hybrid system,[10] have been developed to facilitate large-scale screening and detection of protein–protein interactions *in vivo*.[11,12] Fusion of interacting proteins, each to a different domain of a fragmented transcription factor, will result in transcriptional activation of a reporter if the interaction brings both transcription factor domains into close physical proximity, allowing reconstruction of a functional transcription factor. Although very useful, this system suffers from several drawbacks, including high occurrence of false-positives and the requirement that the interacting proteins accumulate in the cell nucleus.[13] In addition, this system does not preclude indirect interaction of two proteins through a third component present in yeast cells. A different version of the interaction system, the two-hybrid Sos recruitment system, allows identification of cytoplasmic interactions by recruitment of the human Sos protein, a guanyl nucleotide exchange factor, to the cell membrane. At this location, Sos activates the Ras pathway and rescues a temperature-sensitive phenotype of a yeast strain containing a temperature-sensitive mutation in the yeast Sos homolog.[14,15] A variation of this approach, the Ras recruitment system, uses Ras instead of Sos recruitment to the membrane.[16] Another cytoplasmic yeast two-hybrid assay has been developed recently in which reconstitution of N-terminal and C-terminal halves of ubiquitin, when fused to interacting proteins, results in degradation of URA3 reporter protein, resulting in uracil auxotrophy and resistance to 5-fluoroorotic acid.[17] Whereas these methods do not require nuclear import of the interacting proteins, they still suffer from the limitations inherent to yeast-based interaction assays,[18] and they do not allow determination of the native patterns of subcellular localization of the interacting proteins.

A new trend in analyzing protein–protein interactions has emerged with the development of various methods for visualizing proteins in living cells. For example, the interaction between two proteins, each fused to a different and inactive β-galactosidase deletion mutant, has been observed in live mammalian cells.[19,20] The molecular basis for this assay is the ability of inactive β-galactosidase deletion mutants to complement each other *in trans* and to form an active enzyme.[21] While this system allows the *in vivo* detection of protein–protein interactions, its major drawback is the indirect nature of the enzymatic detection assay, which does not allow the user to determine subcellular localization of that interaction accurately.[22] Although more suitable for subcellular localization, this method requires good penetration of substrate into the cell cytoplasm and organelles and, to date, it has been applied only to plant protoplasts.[22]

Other, more direct approaches to investigating protein–protein interactions use changes in fluorescence emissions from fluorescent proteins fused to interacting proteins. For example, the fluorescence resonance energy transfer assay[23,24] allows visualization of protein–protein interactions by fusing interacting proteins to different spectral variants of the green fluorescence protein (GFP). In this approach, the interacting proteins bring their fluorophore tags into close proximity, allowing the transfer of energy from a molecule of an excited donor fluorophore to an acceptor fluorophore molecule without emission of a photon. Following excitation, changes in the second fluorophore's emission intensity can be monitored and attributed to protein–protein interactions. Although useful for detection and for subcellular localization of protein–protein interactions,[25–28] fluorescence resonance energy transfer is technically challenging, as it can be affected by various factors, including autofluorescence and photobleaching, and it requires specialized equipment for fluorescence lifetime imaging as well as special algorithms for data analysis.[23,29]

Recently, a novel approach, termed bimolecular fluorescence complementation (BiFC),[29] has been designed to visualize protein–protein interactions in mammalian cells.[30] BiFC is based on the ability of fusions of interacting proteins to non-fluorescent fragments of the yellow fluorescence protein (YFP) to complement each other and reconstruct a functional YFP.[30] Fragments of YFP can be fused to putative interacting protein partners. If these proteins interact, they may bring together the non-

fluorescing YFP fragments in such a way as to permit refolding of the fluorophore and the subsequent restoration of fluorescence (fluorescence complementation). Initially, BiFC was used to detect interaction and subcellular localization of bZIP and Rel family transcription factors;[30] since then, this method has been implemented for the detection of protein–protein interactions in mammalian cells,[30–33] and in the cells of bacteria,[34,35] and plants.[36–43]

For plant applications, the construction of several expression vectors for detection of protein–protein interaction in the cytoplasm and nucleus of *Arabidopsis* and tobacco cells has been described.[41,42] Although useful, these systems suffer from several limitations, including a rather limited multi-cloning site (MCS), the need to use two selection markers for the production of transgenic plants, and the lack of options for expressing additional genes and/or reporters from the same plasmid.[41,42] To provide these capabilities and help realize the full potential of BiFC in plant research, we designed and constructed a series of vectors that carry constitutive expression cassettes with an expanded MCS (as compared with all BiFC plasmids available to date)[41,42] for easy construction of N-terminal and C-terminal fusions of the target protein to the YFP fragments. This cloning versatility is especially important because reconstruction of the YFP fluorescence requires correct folding and positioning of the interacting fusion proteins, and optimal BiFC often involves testing multiple different combinations and orientations of the target protein-YFP fragment fusions.[29] Furthermore, the design of our vectors allows for assembly of BiFC expression cassettes into *Agrobacterium* multi-gene expression binary plasmids for co-expression of the interacting partners. Finally, these vectors permit the addition of other autofluorescent proteins that may serve as internal transformation controls and markers of subcellular compartments. The compatibility of these vectors with previously described cloning systems provides the user with a versatile collection of interchangeable markers, promoters, and terminators.[44,45]

Results and Discussion

Design of modular satellite plasmids (pSATN) vectors for BiFC

In the BiFC assay, a molecule of YFP is split into two portions, N-terminal (nYFP) and C-terminal (cYFP), neither of which fluoresces on its own; however, when nYFP and cYFP are brought together as fusions with interacting proteins, YFP fluorescence is restored (Figure 1).[30] We utilized the coding sequence of the YFP variant EYFP (Clontech), derived from enhanced GFP (EGFP), which has been codon-optimized for high fluorescence yield in mammalian and plant cells.[46] We

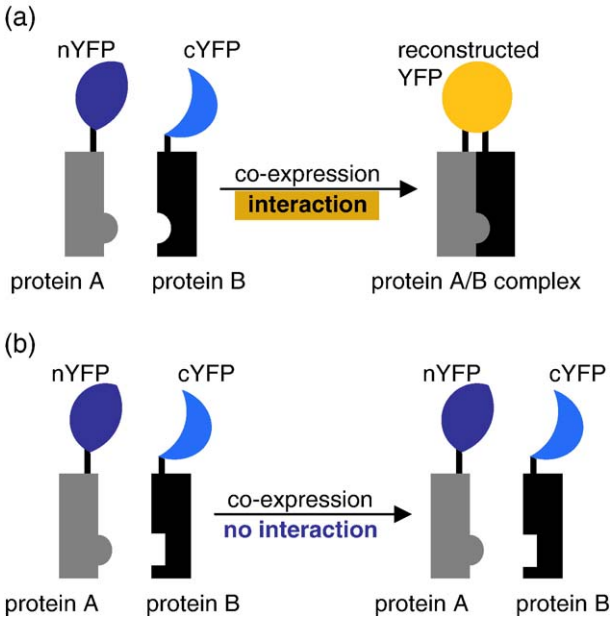

Figure 1. The BiFC assay for detection of protein-protein interactions in living cells. A molecule of an autofluorescent protein reporter, YFP, is split into two parts, N-terminal (nYFP) and C-terminal (cYFP), neither of which fluoresces on its own. Fusion of nYFP and cYFP to tested proteins results in a reconstructed YFP signal (a) if the proteins interact with each other, whereas no YFP fluorescence is produced in the absence of interaction (b).

generated a split between amino acid residues 174 and 175 (N-...Ile-Glu-aSp^{174}/Gly^{175}-Ser-Val...-C) such that the tested proteins are fused to either the N-terminal part of EYFP (nEYFP) or the C-terminal part of EYFP (cEYFP). When the self-interacting protein VirE2, a protein known to multimerize,[47–49] was fused to nEYFP and cEYFP, this 174/175 split resulted in reconstruction of EYFP fluorescence in tobacco BY-2 protoplasts (data not shown). We introduced these nEYFP and cEYFP sequences into sets of pSATN (Figure 2), which allow versatile and simple cloning of the tested genes and assembly of several expression cassettes in a single binary vector for simultaneous expression of multiple genes.[44] The plasmids, illustrated in Figure 2, contain functional plant expression cassettes in which the expression of fused proteins is under the control of the constitutive tandem cauliflower mosaic virus (CaMV) 35S promoter, the tobacco etch virus (TEV) translation leader, and the CaMV 35S poly(A) terminator. We chose these regulatory elements for their ability to promote high expression levels in a wide range of plant species and tissues.[50,51] Both nEYFP and cEYFP were engineered to carry either a stop codon or a translation-initiation codon (ATG), for the C-terminal (C1, Figure 2(a)) or N-terminal (N1, Figure 2(b) and (c)) fusions, respectively. This design allows expression of unfused nEYFP and cEYFP for use as negative controls, as well as production of fusions with genes that lack their own ATG and stop codons.

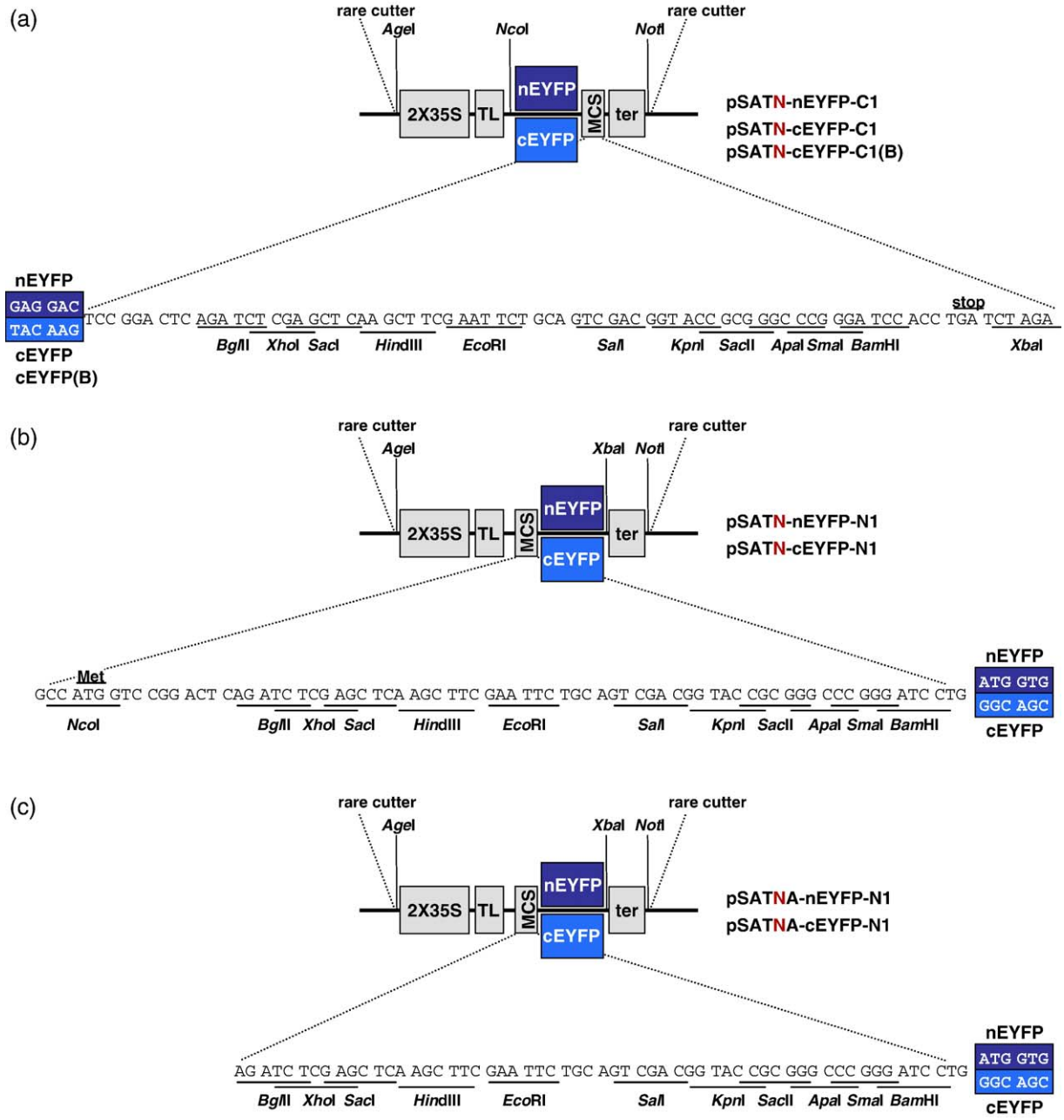

Figure 2. Structural features of the pSATN BiFC series of vectors. The plasmids produce in-frame fusions of the protein of interest to the (a) C terminus or (b) and (c) N terminus of EYFP. Expression cassettes are inserted as AgeI-NotI fragments into three pSATN BiFC plasmids, pSAT1, pSAT 4 and pSAT6, in which the expression cassettes are flanked with unique combinations of rare-cutting endonucleases, i.e. AscI, I-SceI, or PI-PspI for pSAT1, pSAT4, and pSAT6, respectively. Using these rare cutting nucleases, different combinations of the BiFC expression cassettes can be transferred from the pSATN BiFC vectors into the T-DNA region of previously described binary plasmids.[65] Individual pSATN BiFC vectors were designed to allow easy exchange of their promoter and terminator sequences with a larger pSAT family of vectors.[44,45] Open reading frames for nEYFP and cEYFP tags, as well as translation initiation methionine (Met) and stop codons are indicated. Note that the difference between pSATN (b) and pSATNA (c) is in the absence of the NcoI site and its resident ATG codon at the beginning of the multiple cloning site (MCS) in pSATNA. 2X35S, tandem CaMV 35S promoter; TL, TEV translation leader; ter, CaMV 35S poly(A) transcriptional terminator; nEYFP and cEYFP, the N-terminal and C-terminal fragments of EYFP; C1 and N1 vectors produce fusions to the C and N termini of cEYFP and nEYFP, respectively.

Each pSATN BiFC expression construction (Figure 2) was produced in three variations, pSAT1, pSAT4, and pSAT6, in which the expression cassette is flanked by AscI, I-SceI, or PI-PspI rare-cutter recognition sites, respectively.[44,45] Sequence analysis of pSAT6-cEYFP-C1 revealed a cryptic open reading frame (ORF) that could potentially interfere with the correct expression of the cEYFP-tagged

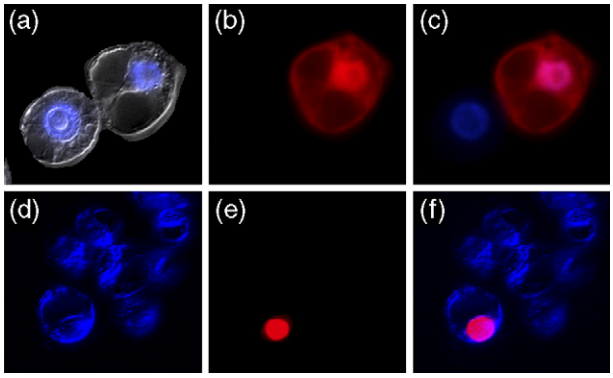

Figure 3. Reference markers for use with BiFC. Free mRFP and mRFP-tagged proteins can be used to detect BY-2 cells that have been transfected. (a) Superimposed images of bright-field and Hoechst 33342 nuclear staining. (b) Free mRFP-expressing transfected cell. (c) Superimposed images of free mRFP and Hoechst 33342 nuclear staining. (d) Bright-field image (pseudo-colored in blue). (e) mRFP-VirD2NLS. (f) Superimposed images of bright-field and mRFP-VirD2NLS.

protein. Therefore, a set of pSATN-cEYFP-C1(B) vectors (Figure 2(a)) was produced in which this cryptic ORF was eliminated.

For easy and versatile cloning, we produced a MCS with 12 unique restriction endonuclease recognition sites (Figure 2). The C1 or N1 fusion MCSs were engineered to produce the same reading frame for each nEYFP and cEYFP pair, thus allowing one-step exchange of fused proteins between each pair of plasmids. To allow for even greater versatility, two more sets of constructs, pSATN(A)-nEYFP-N1 and pSATN(A)-cEYFP-N1, were generated. In these plasmids, the N1 fusion MCS lacks the ATG codon (Figure 2(c)), allowing the user to utilize the tested gene's own ATG as a start codon.

Reference markers for identification of transfected cells and sub-cellular compartments

It is often useful to have a fluorescent marker as an internal reference for cells and subcellular structures when determining protein localization in living cells. Expression of the reference marker additionally helps to identify cells that are transfected and, thus, can be examined for the BiFC signal. We generated constructs to express free, unfused autofluorescent proteins, the enhanced cyan variant of GFP (ECFP) or the monomeric form of DsRed, mRFP.[52] Both of these proteins partition between the cell cytoplasm and the nucleus. In addition, the fluorescence signals of these proteins can be separated easily from those of EYFP, EGFP, chemical dyes and the cells autofluorescence. Figure 3 shows that an mRFP-expressing construct can be effectively used to identify transfected cells (Figure 3(a) and (b)), and it can be employed in conjunction with a chemical dye that stains DNA in the nucleus (Figure 3(c)). We further developed a series of plasmids, in the pSAT6 background, designed to express cDNAs encoding various marker proteins fused to mRFP. Collectively, these reference proteins can be used to identify various sub-cellular compartments‡. Figure 3 shows the localization of mRFP fused to the nuclear localization signal (NLS) of the VirD2 protein of *Agrobacterium* (mRFP-VirD2NLS), to the nuclei of electroporated tobacco BY-2 cells.

BiFC in different sub-cellular compartments

We used the pSATN plasmids to demonstrate the feasibility of the BiFC assay for studying protein–protein interactions in various subcellular compartments of plant cells and in different plant tissues. *Agrobacterium* VirD2 localizes to the nucleus of plant, yeast, and animal cells.[53–56] VirD2 also interacts with the nuclear import-mediator importin α.[57] We generated constructs that tagged VirD2 with nEYFP and the *Arabidopsis* importin α protein AtImpa4 with cEYFP, and co-electroporated them into tobacco BY-2 protoplasts together with a free mRFP-expressing construct. Figure 4(a) shows that nEYFP-tagged VirD2 interacted with cEYFP-tagged AtImpa4 in the cell nucleus. The nuclear localization of the interacting proteins was verified by superimposition (Figure 4(d)) of the YFP signal (Figure 4(a)) over that of the Hoechst 33342 DNA-selective dye (blue fluorescence, Figure 4(b)) and the free mRFP (red fluorescence, Figure 4(c)).

VIP1 dimerizes in the cell nucleus.[38] To demonstrate this specific subcellular interaction and its use with CFP as a reference marker, we co-expressed nEYFP-VIP1 with cEYFP-VIP1 and free ECFP. Figure 4(e) shows that nEYFP-tagged VIP1 interacted with cEYFP-tagged VIP1, and that the resulting BiFC signal was predominantly nuclear. Superimposition of the YFP signal (Figure 4(e)) over that of the co-expressed CFP (Figure 4(f)) and plastid autofluorescence (Figure 4(g)) clearly delineated the expressing cell within the leaf tissue and identified its cytoplasm and nucleus (Figure 4(h)), facilitating the interpretation of the BiFC data.

Next, we examined whether BiFC can be used to detect interactions between proteins within plant intercellular connections, the plasmodesmata.[58] We tested for interaction between the movement protein (MP) of tobacco mosaic virus (TMV) and *Arabidopsis* calreticulin (CRT). These proteins have been shown to interact and localize to plasmodesmata using a fluorescence resonance energy transfer assay.[28] Figure 5(a) shows that co-expression of CRT tagged with cEYFP and TMV MP tagged with nEYFP resulted in fluorescence complementation within distinct puncta at the cell periphery of *Nicotiana benthamiana* cells, a pattern characteristic of plasmodesmal localization.[59–62] No signal was observed following cobombardment of nEYFP-tagged TMV MP with free cEYFP (data not shown).

‡http://www.biology.purdue.edu/people/faculty/gelvin/nsf/index.htm

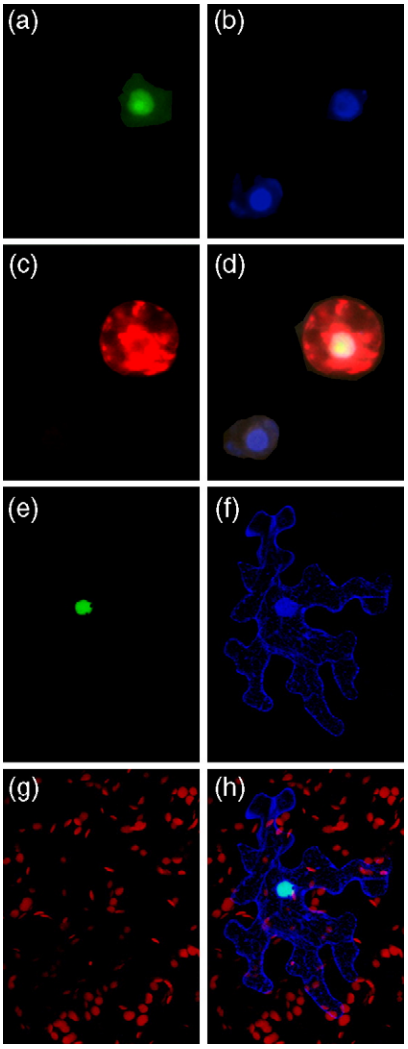

Figure 4. The use of a chemical dye, CFP and mRFP as internal markers during BiFC detection of protein-protein interactions. (a)–(d) Interaction between cEYFP-tagged AtImpa4 and nEYFP-tagged VirD2 in BY-2 protoplasts. (a) The images of the reconstructed YFP signal, (b) nuclear staining by the DNA-selective dye Hoechst 33342 and (c) co-expressed free mRFP were (d) superimposed to better demonstrate the nuclear location of the interacting proteins. (e) to (h) Dimerization of nEYFP-tagged and cEYFP-tagged VIP1 in the *N. benthamiana* cell nucleus. (e) The images of the reconstructed YFP signal, (f) co-expressed free ECFP, and (g) plastid autofluorescence were (f) superimposed to better demonstrate the nuclear location of the interacting proteins.

Co-expressed autofluorescent proteins can be used as markers for specific subcellular compartments and organelles when fused to proteins that target to such compartments. Colocalization of such specific reference markers with the BiFC signal helps to identify the subcellular location of the interacting proteins. We illustrated this concept in a BiFC assay of protein–protein interactions between subunits of a cucumber chromoplast D (ChrD) protein. This protein localizes to plastids and dimerizes.[63,64] We co-expressed nEYFP-tagged ChrD and cYFP-tagged ChrD in *Arabidopsis* leaves with ChrD fused to mRFP. Because all pSATN BiFC vectors are compatible with our previously described modular system for expressing multiple genes in plants,[44,45] we mounted all three expression constructs onto a single *Agrobacterium* binary plasmid pPZP-RCS2.[65] Figure 5(b) to (e) exemplifies the imaging of a typical cell expressing all three fusion proteins, where both expression of mRFP-tagged ChrD (Figure 5(b)) and reconstruction of the YFP signal due to BiFC following ChrD dimerization (Figure 5(c)) are observed in the background of plastid autofluorescence (Figure 5(d)). Merging all three images confirmed the expected localization of the ChrD-ChrD dimers within the cell chloroplasts identified by the presence of mRFP-tagged ChrD (Figure 5(e)).

BiFC in different plant tissues and cell types

BiFC has been demonstrated in several plant species, including *Arabidopsis thaliana*,[42] tobacco (*Nicotiana tobacum*),[37,41,42] onion (*Allium cepa*),[37,39] and parsley (*Petroselinum crispum*),[40] using various transformation techniques. In addition to leaf tissues and tobacco protoplasts (Figures 4 and 5), we examined the functionality of our BiFC vectors in

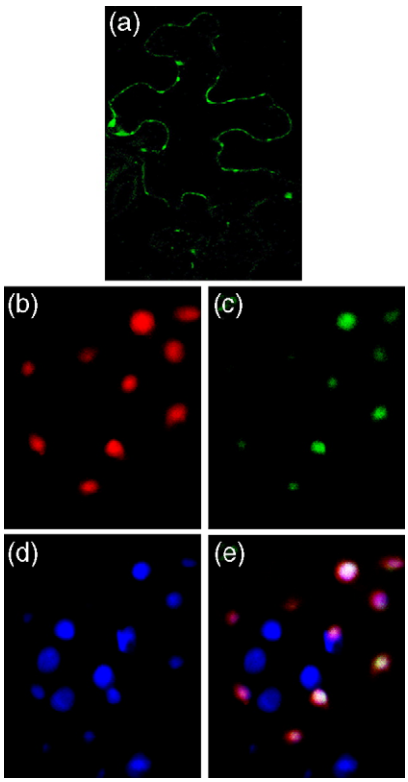

Figure 5. BiFC detection of protein-protein interactions in different sub-cellular locations. (a) Interaction between nEYFP-tagged TMV MP and cEYFP-tagged CRT in plasmodesmata of tobacco leaves. (b) to (e) Dimerization of nEYFP- and cEYFP-tagged ChrD in chloroplasts of *Arabidopsis* leaf cells. (b) The images of the reconstructed YFP signal, (c) co-expressed mRFP-tagged ChrD, and (d) plastid autofluorescence were (e) superimposed to identify the plastid location of the interacting proteins.

several other plant cells and model systems. In these experiments, we utilized dimerization of the tomato yellow leaf curl virus (TYLCV) capsid protein (CP). Interaction of cEYFP-tagged TYLCV CP with nEYFP-tagged TYLCV CP was detected within the nucleus of a tomato leaf mesophyll cell (Figure 6(a)) against the background of plastid autofluorescence (Figure 6(b)). This observation is consistent with previous reports that TYLCV CP is a nuclear protein[66] capable of homotypic oligomerization.[67] The use of differential interference contrast (DIC) confocal imaging allowed visualization of the cell nucleus in DIC (Figure 6(c), arrow), and superimposition of the fluorescence and bright-field images confirmed the localization of the CP–CP complex (Figure 6(d)). Dimerization of TYLCV CP within the cell nucleus was observed also in tomato leaf trichome cells (Figure 6(e) to (h)) as well as in isolated tobacco leaf protoplasts (Figure 6(i) to (l)). Notably, trichomes and protoplasts are often used as experimental systems for virus–host plant interactions,[68–71] making BiFC useful for such studies. BiFC can also be used to visualize protein–protein interactions in onion epidermal cells. Importin α molecules can dimerize,[72] and can be detected by BiFC to colocalize with the nuclear portion of the co-expressed internal reference fluorescence marker, mRFP (Figure 6(m)).

Confocal microscopy is the tool of choice for detailed, high-resolution analyses of fluorescently tagged proteins in living cells.[73,74] Nevertheless, epifluorescence microscopy is still widely used as a simple and low-cost alternative for visualization of intracellular fluorescence. We tested the applicability of our BiFC vectors, in combination with reference autofluorescent protein markers or fluorescent dyes, for detection of BiFC by epifluorescence microscopy (Figures 4(a)–(d), and 6(n) and (o)). Importin α molecules from *Arabidopsis* dimerize in tobacco BY-2 cells. In Figure 6(n), the reconstructed YFP signal was initially merged with a bright-field whole-cell image (pseudo-colored in blue) to localize the dimerized proteins to what appeared to be the cell nucleus. Nuclear localization of importin α dimers in a different image was confirmed by co-localization of the reconstructed YFP signal with the DNA-selective dye Hoechst 33242 (Figure 6(o)).

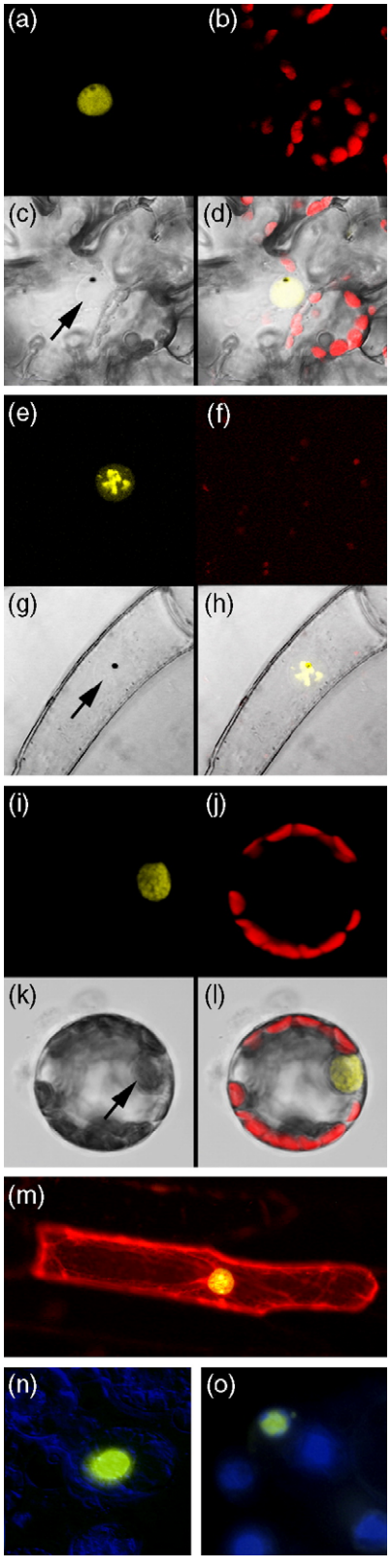

Figure 6. BiFC detection of protein–protein interactions in different plant tissues and cell types. Dimerization of nEYFP-tagged and cEYFP-tagged TYLCV CP in the nuclei of (a) to (d) tomato mesophyll cells, (e) to (h) tomato trichomes and (i)–(l) isolated tobacco leaf protoplasts. The images of (a), (e), and (i) the reconstructed YFP signal, (b), (f), and (j), plastid autofluorescence, and (c), (g), and (k) DIC were (d), (h), and (l) superimposed to better demonstrate the nuclear location of the interacting proteins. Arrows point to the location of the cell nucleus in DIC images. YFP signal is in yellow and plastid autofluorescence is in red. (m) Dimerization of nEYFP- and cEYFP-tagged importin α in onion epidermal cells. The BiFC YFP signal is superimposed upon the mRFP expressing cell. Fluorescence images are single confocal sections. (n) to (o) Dimerization of nEYFP-tagged and cEYFP-tagged importin α in tobacco BY-2 protoplasts. (n) The BiFC YFP signal is superimposed with bright-field image (pseudo-colored in blue). (o) The superimposition of the YFP signal (yellow) with Hoechst 33342 DNA-selective dye (blue) allowed better identification of the cell nucleus in epifluorescence images.

Here, we describe a new series of modular vectors designed to carry out BiFC assays in plant cells. The functionality of these vectors was demonstrated with a wide range of interacting proteins derived from different plant species as well as from plant bacterial and viral pathogens, and protein–protein interactions were detected in diverse plant species, tissues and cell types, and isolated protoplasts. Importantly, BiFC allowed detection of protein–protein interactions in various subcellular compartments, from the cell nucleus to plasmodesmata to chloroplasts. We showed the applicability of our vector system in conjunction with coexpression of reference autofluorescent protein markers, such as CFP and mRFP, and with the fluorescent dye Hoechst 33242. Protein–protein interactions were visualized using both confocal and epifluorescence microscopy, and the transformation of plant tissues and cells with our vectors was achieved using diverse transformation techniques. Thus, our BiFC vectors are suitable for studies of protein–protein interactions in a wide range of plant species, tissues, and cell types, as well as for different transformation and detection techniques, from more costly microbombardment and confocal microscopy to cost-effective agroinfiltration and epifluorescence microscopy.

A useful feature of our BiFC vectors is their compatibility with a larger family of plasmids for the cloning and expression of multiple genes.[44,45] With this system, genes, promoters, terminators, and complete expression cassettes can be shuttled easily between plasmids and multiple expression cassettes. BiFC components and reference markers can be assembled onto a single *Agrobacterium* binary plasmid. This capability is unique to the pSATN BiFC vectors, and it is not available with other BiFC vectors.[41,42] Further, users who are interested in performing BiFC in transgenic plants can choose between three selection markers (*bar*, *nptII*, and *hpt*)[44,45] when mounting their BiFC expression cassettes and fluorescent markers onto binary vectors. Complete sequences of all our pSATN BiFC vectors as well as of the multi-gene expression binary plasmids are available both from GenBank and at our website§.

Experimental Procedures

Plasmid construction

For production of pSATN BiFC vectors, the original MCS of pUC18[75] was replaced using PCR with the following forward and reverse primers: 5′AAATACTGCAGCCATGGAATTCTAGAGCGGCCGCGTAATCATGGTCATAGCTGTTTCC3′ and 5′AAATACTGCAGGTCGACGAATTCACCGGTGGCACTGGCCGTCGTTTTACAACG3′. The PCR product was digested with PstI and self-ligated, resulting in pUC18-MCS-A, which contains the following restriction endonuclease recognition sites: AgeI, EcoRI, SalI, PstI, NcoI, EcoRI, XbaI and NotI. To assemble a functional plant expression cassette, the tandem CaMV 35S promoter was PCR-amplified from pRTL2-GUS,[51] and inserted into the AgeI-SalI sites of pUC18-MCS-A, producing pUC18-2x35Sp. Next, the TEV translation leader, TL, was PCR-amplified from pRTL2-GUS and cloned into the XhoI-NcoI sites of pUC18-2x35Sp, producing pUC18-2x35Sp-TL. A single A to G mutation was introduced into one of the TL primers in order to eliminate an internal EcoRI site located at the 5′end of the TL sequence. Finally, the entire EYFP ORF and its adjacent MCS and the 35S poly(A) terminator were PCR-amplified from pEYFP-C1 (Clontech) and pRTL2-GUS, respectively, and cloned by triple ligation as EYFP-MCS NcoI-XbaI and 35 S poly(A) XbaI-NotI fragments into the NcoI-NotI sites of pUC18-2x35Sp-TL, producing a vector with a complete EYFP-C1 expression cassette, designated pSAT-EYFP-C1. The EYFP-C1 expression cassette was then transferred as an AgeI-NcoI fragment into pAUX3133,[65] creating pSAT6-EYFP-C1. Then, the YFP ORF from pSAT6-EYFP-C1 was replaced with NcoI-XhoI PCR products corresponding to the N-terminal (amino acid residues 1–174, nEYFP) and C-terminal (amino acid residues 175–239, cEYFP) of EYFP, to produce pSAT6-cEYFP-C1 and pSAT6-nEYFP-C1, respectively, while maintaining the original EYFP MCS and reading frame. To eliminate a cryptic ORF found in pSAT6-cEYFP-C1, nEYFP was PCR-amplified to encode an extra glycine residue at position 3, while eliminating the additional ATG in pSAT6-cEYFP-C1 and producing pSAT6-cEYFP-C1(B).

The entire MCS and its adjacent 35 S poly(A) were PCR-amplified from pSAT6-EYFP-C1 and cloned into the NcoI-NotI sites of pUC18-2x35Sp-TL, creating the plant expression vector pSAT-MCS, from which the empty expression cassette was transferred as an AgeI-NcoI fragment into pAUX3133, creating pSAT6-MCS. To produce pSAT6-nEYFP-N1 and pSAT6-cEYFP-N1, SalI-BglII PCR fragments of nEYFP and cEYFP, respectively, were cloned into the SalI-BamHI sites of pSAT6-MCS. To eliminate the NcoI site and its cryptic translation initiation site, the AgeI-BglII fragments, containing the tandem 35 S promoter and its adjacent TL enhancer in pSAT6(A)-cEYFP-N1 and pSAT6(A)-nEYFP-N1, were replaced by a modified (lacking the NcoI site) promoter fragment from pSAT6(A)-EGFP-N1,[45] creating pSAT(A)-cEYFP-N1 and pSAT(A)-nEYFP-N1, respectively.

Finally, the BiFC expression cassettes from pSAT6-cEYFP-C1, pSAT6-cEYFP-C1(B), pSAT6-nEYFP-C1, pSAT6-cEYFP-N1 and pSAT6-nEYFP-N1 were transferred as AgeI-NcoI fragments into pAUX3166,[65] creating pSAT1-cEYFP-C1, pSAT1-cEYFP-C1(B), pSAT1-nEYFP-C1, pSAT1-cEYFP-N1 and pSAT1-nEYFP-N1, respectively, and into pAUX3131,[65] creating pSAT4-cEYFP-C1, pSAT4-cEYFP-C1(B), pSAT4-nEYFP-C1, pSAT4-cEYFP-N1 and pSAT4-nEYFP-N1, respectively. All PCR reactions were performed using a high-fidelity *Pfu* DNA polymerase (Stratagene), and their products were verified by DNA sequencing. Structural features of the pSATN BiFC vectors are shown in Figure 2.

Genes encoding all tested proteins were cloned into the MCS of different pSATN BiFC vectors as follows. The AtImpa4 ORF was PCR-amplified and cloned into KpnI-XmaI sites of pGEM-T-Easy. The ORF was subsequently excised using NcoI and XmaI, and ligated into the corresponding sites of pSAT6-cEYFP-N1, generating pSAT6-AtImpa4-cYFP. The VirD2 gene was PCR-amplified and cloned into the SmaI site of pBluescript. The ORF was subsequently excised using EcoRI and SacII, and

§ http://www.biology.purdue.edu/people/faculty/gelvin/nsf/index.htm

ligated into the corresponding sites of pSAT6-nEYFP-C1, generating pSAT6-nEYFP-VirD2. The *Arabidopsis* calreticulin *CRT1*[28] was PCR-amplified and cloned into the SalI-BamHI sites of pSAT6-cEYFP-N1, and PCR-amplified TMV MP sequence[76] was cloned into the EcoRI-SalI sites of pSAT6-nEYFP-N1, producing pSAT6-CRT1-cEYFP and pSAT6-TMV-MP-nEYFP, respectively. The *Arabidopsis VIP1* gene[77] was transferred as a SalI-BamHI fragment from pSAT6-EGFP-VIP1[44] into the same sites of pSAT1-cEYFP-C1(B) and pSAT4-nEYFP-C1, producing pSAT1-cEYFP-VIP1 and pSAT4-nEYFP-VIP1, respectively. The tomato *chrD* gene[63] was PCR-amplified and cloned into the SalI-BamHI sites of pSAT4(A)-nEYFP-N1, pSAT1(A)-cEYFP-N1, and pSAT6(A)-mRFP-N1, producing pSAT4(A)-chrD-nEYFP, pSAT1(A)-chrD-cEYFP and pSAT6(A)-chrD-mRFP-N1, respectively; for multigene expression, their expression cassettes were transferred into the I-SceI, AscI and PI-PspI sites pf pPZP-RCS2,[44,65] producing pPZP-RCS2-chrD-BiFC. The TYLCV CP sequence[66] was PCR-amplified and cloned into the XhoI-BamHI sites of pSAT4-nEYFP-C1 and pSAT1-cEYFP-C1, producing pSAT4-nEYFP-TYLCV CP and pSAT1-cEYFP-TYLCV CP, respectively. The NLS sequence of *virD2*[78] was excised as a KpnI-HincII fragment from pUC118-VirD2 and cloned into the KpnI and SmaI sites of pSAT6-mRFP-C1.

Transformation of plant tissues

For microbombardment experiments, various combinations of plasmids encoding cEYFP and nEYFP fusion proteins were mixed at a 1:1 (w/w) ratio and 50 μg of DNA was adsorbed onto 10 μg of 1 μm gold particles according to the manufacturer's instructions (Bio-Rad). The particles were microbombarded into the leaf epidermis of greenhouse-grown *Nicotiana benthamiana* or tomato (*Solanum lycopersicum*) plants or onion epidermal peels. Microbombardment was performed at a pressure of 150 psi (1 psi ≈6.9 kPa) using a portable Helios gene gun system (model PDS-1000/He, Bio-Rad), and tissues were analyzed 16–24 h after bombardment. For agroinfiltration, binary plasmids were mobilized into *Agrobacterium tumefaciens* as described,[79] grown overnight at 25 °C, and infiltrated into intact *N. benthamiana* and *Arabidopsis* leaves, as described.[80,81] Infected tissues were analyzed at 16–24 h after agroinfiltration. For protoplast transformation, leaf mesophyll protoplasts were isolated from *N. tabacum* L. cv. *Samsun* NN as described,[82] and a mixture of 5 μg of plasmid DNA and 15 μg of calf thymus DNA was used for electroporation of 0.5 ml of protoplast solution as described.[83] Transformed protoplasts were incubated in the dark for 46–48 h at 27 °C prior to imaging. Tobacco BY-2 suspension cell protoplasts were generated and transfected as described.[56]

Confocal and epifluorescence microscopy

Plant tissues were viewed directly under a Zeiss LSM 5 Pascal confocal laser-scanning microscope equipped with two laser lines and a set of filters capable of distinguishing between the cyan (ECFP), yellow (EYFP) and red (mRFP) fluorescence proteins and plastid autofluorescence, or under an OLYMPUS IX 81 confocal laser-scanning microscope equipped with a single laser line and a set of filters capable of distinguishing between EYFP and plastid autofluorescence, as well as with a Nomarski differential interference contrast (DIC) lens for capturing transmitted light images. For epifluorescence microscopy, cells were stained with Hoechst 33342 (final concentration, 20 ng/ml) 10 min before observation and were imaged using a NIKON ECLIPSE E600 epifluorescence microscope equipped with YFP-, RFP- (HcRed) and UV-specific filters.

Database accession numbers

The complete sequences of the pSATN BiFC vectors have been deposited in GenBank (accession numbers DQ169005, DQ169004, DQ169003, DQ169002, DQ169001, DQ169000, DQ168999, DQ168998, DQ168997, DQ168996, DQ168995 and DQ168994 for pSAT4-nEYFP-N1, pSAT4-cEYFP-N1, pSAT4(A)-nEYFP-N1, pSAT4(A)-cEYFP-N1, pSAT1-nEYFP-N1, pSAT1-cEYFP-N1, pSAT1(A)-nEYFP-N1, pSAT1(A)-cEYFP-N1, pSAT4-cEYFP-C1(B), pSAT1-cEYFP-C1(B), pSAT1-nEYFP-C1 and pSAT4-nEYFP-C1, respectively) and the vectors are freely available to the plant research community.

Acknowledgements

The work in our laboratories is supported by grants from NIH, USDA, and BSF to V.C., from the NSF 2010 Program to S.B.G. and V.C. (MCB-0418709), from BARD to V.C. and Y.G., and from BARD to T.T. We thank Sergei Kraznyanski and Kelly Babb for technical assistance.

References

1. Weis, K. (2003). Regulating access to the genome. Nucleocytoplasmic transport throughout the cell cycle. *Cell*, **112**, 441–451.
2. Lehmann, M. (2004). Anything else but GAGA: a nonhistone protein complex reshapes chromatin structure. *Trends Genet.* **20**, 15–22.
3. Ogata, K., Sato, K., Tahirov, T. H. & Tahirov, T. (2003). Eukaryotic transcriptional regulatory complexes: cooperativity from near and afar. *Curr. Opin. Struct. Biol.* **13**, 40–48.
4. Tzfira, T. & Citovsky, V. (2002). Partners-in-infection: host proteins involved in the transformation of plant cells by *Agrobacterium*. *Trends Cell Biol.* **12**, 121–129.
5. Heyl, A. & Schmulling, T. (2003). Cytokinin signal perception and transduction. *Curr. Opin. Plant Biol.* **6**, 480–488.
6. Immink, R. G. & Angenent, G. C. (2002). Transcription factors do it together: the hows and whys of studying protein-protein interactions. *Trends Plant Sci.* **7**, 531–534.
7. Phizicky, E. M. & Fields, S. (1995). Protein-protein interactions: methods for detection and analysis. *Microbiol. Rev.* **59**, 94–123.
8. Gu, W., Schneider, J. W., Condorelli, G., Kaushal, S., Mahdavi, V. & Nadal-Ginard, B. (1993). Interaction of myogenic factors and the retinoblastoma protein mediates muscle cell commitment and differentiation. *Cell*, **72**, 309–324.
9. Halevy, O., Novitch, B. G., Spicer, D. B., Skapek, S. X., Rhee, J., Hannon, G. J. *et al.* (1995). Correlation of

terminal cell cycle arrest of skeletal muscle with induction of p21 by MyoD. *Science*, **267**, 1018–1021.
10. Fields, S. & Song, O.-K. (1989). A novel genetic system to detect protein-protein interactions. *Nature*, **340**, 245–246.
11. Causier, B. & Davies, B. (2002). Analysing protein-protein interactions with the yeast two-hybrid system. *Plant Mol. Biol.* **50**, 855–870.
12. Fromont-Racine, M., Mayes, A. E., Brunet-Simon, A., Rain, J. C., Colley, A., Dix, I. *et al.* (2000). Genome-wide protein interaction screens reveal functional networks involving Sm-like proteins. *Yeast*, **17**, 95–110.
13. Golemis, E. A., Serebriiskii, I. & Law, S. F. (1999). The yeast two-hybrid system: criteria for detecting physiologically significant protein-protein interactions. *Curr. Issues Mol. Biol.* **1**, 31–45.
14. Aronheim, A., Zandi, E., Hennemann, H., Elledge, S. J. & Karin, M. (1997). Isolation of an AP-1 repressor by a novel method for detecting protein- protein interactions. *Mol. Cell. Biol.* **17**, 3094–3102.
15. Maroun, M. & Aronheim, A. (1999). A novel *in vivo* assay for the analysis of protein-protein interaction. *Nucl. Acids Res.* **27**, e4.
16. Broder, Y. C., Katz, S. & Aronheim, A. (1998). The Ras recruitment system, a novel approach to the study of protein–protein interactions. *Curr. Biol.* **8**, 1121–1124.
17. Deslandes, L., Olivier, J., Peeters, N., Feng, D. X., Khounlotham, M., Boucher, C. *et al.* (2003). Physical interaction between RRS1-R, a protein conferring resistance to bacterial wilt, and PopP2, a type III effector targeted to the plant nucleus. *Proc. Natl Acad. Sci. USA*, **100**, 8024–8029.
18. Fields, S. (2005). High-throughput two-hybrid analysis. The promise and the peril. *FEBS J.* **272**, 5391–5399.
19. Rossi, F., Charlton, C. A. & Blau, H. M. (1997). Monitoring protein-protein interactions in intact eukaryotic cells by beta-galactosidase complementation. *Proc. Natl Acad. Sci. USA*, **94**, 8405–8410.
20. Rossi, F. M., Blakely, B. T., Charlton, C. A. & Blau, H. M. (2000). Monitoring protein-protein interactions in live mammalian cells by beta-galactosidase complementation. *Methods Enzymol.* **328**, 231–251.
21. Mohler, W. A. & Blau, H. M. (1996). Gene expression and cell fusion analyzed by lacZ complementation in mammalian cells. *Proc. Natl Acad. Sci. USA*, **93**, 12423–12427.
22. Subramaniam, R., Desveaux, D., Spickler, C., Michnick, S. W. & Brisson, N. (2001). Direct visualization of protein interactions in plant cells. *Nature Biotechnol.* **19**, 769–772.
23. Sekar, R. B. & Periasamy, A. (2003). Fluorescence resonance energy transfer (FRET) microscopy imaging of live cell protein localizations. *J. Cell Biol.* **160**, 629–633.
24. Day, R. N., Periasamy, A. & Schaufele, F. (2001). Fluorescence resonance energy transfer microscopy of localized protein interactions in the living cell nucleus. *Methods*, **25**, 4–18.
25. Del Pozo, M. A., Kiosses, W. B., Alderson, N. B., Meller, N., Hahn, K. M. & Schwartz, M. A. (2002). Integrins regulate GTP-Rac localized effector interactions through dissociation of Rho-GDI. *Nature Cell Biol.* **4**, 232–239.
26. Elangovan, M., Day, R. N. & Periasamy, A. (2002). Nanosecond fluorescence resonance energy transfer-fluorescence lifetime imaging microscopy to localize the protein interactions in a single living cell. *J. Microsc.* **205**, 3–14.
27. Elangovan, M., Wallrabe, H., Chen, Y., Day, R. N., Barroso, M. & Periasamy, A. (2003). Characterization of one- and two-photon excitation fluorescence resonance energy transfer microscopy. *Methods*, **29**, 58–73.
28. Chen, M. H., Tian, G. W., Gafni, Y. & Citovsky, V. (2005). Effects of calreticulin on viral cell-to-cell movement. *Plant Physiol.* **138**, 1866–1876.
29. Bhat, R. A., Lahaye, T. & Panstruga, R. (2006). The visible touch: in planta visualization of protein-protein interactions by fluorophore-based methods. *Plant Methods*, **2**, 12.
30. Hu, C. D., Chinenov, Y. & Kerppola, T. K. (2002). Visualization of interactions among bZIP and Rel family proteins in living cells using bimolecular fluorescence complementation. *Mol. Cell*, **9**, 789–798.
31. Hu, C. D. & Kerppola, T. K. (2003). Simultaneous visualization of multiple protein interactions in living cells using multicolor fluorescence complementation analysis. *Nature Biotechnol.* **21**, 539–545.
32. Hynes, T. R., Tang, L., Mervine, S. M., Sabo, J. L., Yost, E. A., Devreotes, P. N. & Berlot, C. H. (2004). Visualization of G protein beta gamma dimers using bimolecular fluorescence complementation demonstrates roles for both beta and gamma in subcellular targeting. *J. Biol. Chem.* **279**, 30279–30286.
33. Grinberg, A. V., Hu, C. D. & Kerppola, T. K. (2004). Visualization of Myc/Max/Mad family dimers and the competition for dimerization in living cells. *Mol. Cell. Biol.* **24**, 4294–4308.
34. Atmakuri, K., Ding, Z. & Christie, P. J. (2003). VirE2, a type IV secretion substrate, interacts with the VirD4 transfer protein at cell poles of *Agrobacterium tumefaciens*. *Mol. Microbiol.* **49**, 1699–1713.
35. Tsuchisaka, A. & Theologis, A. (2004). Heterodimeric interactions among the 1-amino-cyclopropane-1-carboxylate synthase polypeptides encoded by the *Arabidopsis* gene family. *Proc. Natl Acad. Sci. USA*, **101**, 2275–2280.
36. Lacroix, B., Vaidya, M., Tzfira, T. & Citovsky, V. (2005). The VirE3 protein of *Agrobacterium* mimics a host cell function required for plant genetic transformation. *EMBO J.* **24**, 428–437.
37. Tzfira, T., Vaidya, M. & Citovsky, V. (2004). Involvement of targeted proteolysis in plant genetic transformation by *Agrobacterium*. *Nature*, **431**, 87–92.
38. Li, J., Krichevsky, A., Vaidya, M., Tzfira, T. & Citovsky, V. (2005). Uncoupling of the functions of the *Arabidopsis* VIP1 protein in transient and stable plant genetic transformation by *Agrobacterium*. *Proc. Natl Acad. Sci. USA*, **102**, 5733–5738.
39. Diaz, I., Martinez, M., Isabel-LaMoneda, I., Rubio-Somoza, I. & Carbonero, P. (2005). The DOF protein, SAD, interacts with GAMYB in plant nuclei and activates transcription of endosperm-specific genes during barley seed development. *J. Plant*, **42**, 652–662.
40. Stolpe, T., Susslin, C., Marrocco, K., Nick, P., Kretsch, T. & Kircher, S. (2005). In planta analysis of protein-protein interactions related to light signaling by bimolecular fluorescence complementation. *Protoplasma*, **226**, 137–146.
41. Walter, M., Chaban, C., Schütze, K., Batistic, O., Weckermann, K., Näke, C. *et al.* (2004). Visualization of protein interactions in living plant cells using bimolecular fluorescence complementation. *J. Plant*, **40**, 428–438.

42. Bracha-Drori, K., Shichrur, K., Katz, A., Oliva, M., Angelovici, R., Yalovsky, S. & Ohad, N. (2004). Detection of protein-protein interactions in plants using bimolecular fluorescence complementation. *J. Plant*, **40**, 419–427.
43. Abe, M., Kobayashi, Y., Yamamoto, S., Daimon, Y., Yamaguchi, A., Ikeda, Y. *et al.* (2005). FD, a bZIP protein mediating signals from the floral pathway integrator FT at the shoot apex. *Science*, **309**, 1052–1056.
44. Tzfira, T., Tian, G.-W., Lacroix, B., Vyas, S., Li, J., Leitner-Dagan, Y. *et al.* (2005). pSAT vectors: a modular series of plasmids for autofluorescent protein tagging and expression of multiple genes in plants. *Plant Mol. Biol.* **57**, 503–516.
45. Chung, S. M., Frankman, E. L. & Tzfira, T. (2005). A versatile vector system for multiple gene expression in plants. *Trends Plant Sci.* **10**, 357–361.
46. Yang, T. T., Cheng, L. & Kain, S. R. (1996). Optimized codon usage and chromophore mutations provide enhanced sensitivity with the green fluorescent protein. *Nucl. Acids Res.* **24**, 4592–4593.
47. Citovsky, V., Wong, M. L. & Zambryski, P. C. (1989). Cooperative interaction of *Agrobacterium* VirE2 protein with single stranded DNA: implications for the T-DNA transfer process. *Proc. Natl Acad. Sci. USA*, **86**, 1193–1197.
48. Zhou, X. R. & Christie, P. J. (1999). Mutagenesis of the *Agrobacterium* VirE2 single-stranded DNA-binding protein identifies regions required for self-association and interaction with VirE1 and a permissive site for hybrid protein construction. *J. Bacteriol.* **181**, 4342–4352.
49. Dombek, P. & Ream, L. W. (1997). Functional domains of *Agrobacterium tumefaciens* single-stranded DNA-binding protein VirE2. *J. Bacteriol.* **179**, 1165–1173.
50. Hull, R., Covey, S. N. & Dale, P. (2002). Genetically modified plants and the 35S promoter: assessing the risk and enhancing the debate. *Microb. Ecol. Health Dis.* **12**, 1–5.
51. Restrepo, M. A., Freed, D. D. & Carrington, J. C. (1990). Nuclear transport of plant potyviral proteins. *Plant Cell*, **2**, 987–998.
52. Shaner, N. C., Campbell, R. E., Steinbach, P. A., Giepmans, B. N., Palmer, A. E. & Tsien, R. Y. (2004). Improved monomeric red, orange and yellow fluorescent proteins derived from Discosoma sp. red fluorescent protein. *Nature Biotechnol.* **22**, 1567–1572.
53. Howard, E. A., Zupan, J. R., Citovsky, V. & Zambryski, P. C. (1992). The VirD2 protein of A. *tumefaciens* contains a C-terminal bipartite nuclear localization signal: implications for nuclear uptake of DNA in plant cells. *Cell*, **68**, 109–118.
54. Koukolikova-Nicola, Z., Raineri, D., Stephens, K., Ramos, C., Tinland, B., Nester, E. W. & Hohn, B. (1993). Genetic analysis of the virD operon of *Agrobacterium tumefaciens*: a search for functions involved in transport of T-DNA into the plant cell nucleus and in T-DNA integration. *J. Bacteriol.* **175**, 723–731.
55. Guralnick, B., Thomsen, G. & Citovsky, V. (1996). Transport of DNA into the nuclei of *Xenopus* oocytes by a modified VirE2 protein of *Agrobacterium*. *Plant Cell*, **8**, 363–373.
56. Mysore, K. S., Bassuner, B., Deng, X.-B., Darbinian, N. S., Motchoulski, A., Ream, L. W. & Gelvin, S. B. (1998). Role of the *Agrobacterium tumefaciens* VirD2 protein in T-DNA transfer and integration. *Mol. Plant-Microbe Interact.* **11**, 668–683.
57. Ballas, N. & Citovsky, V. (1997). Nuclear localization signal binding protein from *Arabidopsis* mediates nuclear import of *Agrobacterium* VirD2 protein. *Proc. Natl Acad. Sci. USA*, **94**, 10723–10728.
58. Lucas, W. J. & Lee, J. Y. (2004). Plasmodesmata as a supracellular control network in plants. *Nature Rev. Mol. Cell Biol.* **5**, 712–726.
59. Baluska, F., Cvrckova, F., Kendrick-Jones, J. & Volkmann, D. (2001). Sink plasmodesmata as gateways for phloem unloading. Myosin VIII and calreticulin as molecular determinants of sink strength? *Plant Physiol.* **126**, 39–46.
60. Baluska, F., Samaj, J., Napier, R. & Volkmann, D. (1999). Maize calreticulin localizes preferentially to plasmodesmata in root apex. *J. Plant*, **19**, 481–488.
61. Laporte, C., Vetter, G., Loudes, A. M., Robinson, D. G., Hillmer, S., Stussi-Garaud, C. & Ritzenthaler, C. (2003). Secretory pathway and the cytoskeleton in intracellular targeting and tubule assembly of Grapevine fanleaf virus movement protein in tobacco BY-2 cells. *Plant Cell*, **15**, 2058–2075.
62. Oparka, K. J., Prior, D. A. M., Santa-Cruz, S., Padgett, H. S. & Beachy, R. N. (1997). Gating of epidermal plasmodesmata is restricted to the leading edge of expanding infection sites of tobacco mosaic virus (TMV). *J. Plant*, **12**, 781–789.
63. Libal-Weksler, Y., Vishnevetsky, M., Ovadis, M. & Vainstein, A. (1997). Isolation and regulation of accumulation of a minor chromoplast-specific protein from cucumber corollas. *Plant Physiol.* **113**, 59–63.
64. Leitner-Dagan, Y., Ovadis, M., Zuker, A., Shklarman, E., Ohad, I., Tzfira, T. & Vainstein, A. (2006). CHRD, a plant member of the evolutionary conserved YjgF family, influences photosyntheis and chromoplastogenesis. *Planta* (in press).
65. Goderis, I. J., De Bolle, M. F., Francois, I. E., Wouters, P. F., Broekaert, W. F. & Cammue, B. P. (2002). A set of modular plant transformation vectors allowing flexible insertion of up to six expression units. *Plant Mol. Biol.* **50**, 17–27.
66. Kunik, T., Palanichelvam, K., Czosnek, H., Citovsky, V. & Gafni, Y. (1998). Nuclear import of the capsid protein of tomato yellow leaf curl virus (TYLCV) in plant and insect cells. *J. Plant*, **13**, 393–399.
67. Hallan, V. & Gafni, Y. (2001). Tomato yellow leaf curl virus (TYLCV) capsid protein (CP) subunit interactions: implications for viral assembly. *Arch. Virol.* **146**, 1765–1773.
68. Derrick, P. M., Barker, H. & Oparka, K. J. (1992). Increase in plasmodesmatal permeability during cell-to-cell spread of tobacco rattle tobravirus from individually inoculated cells. *Plant Cell*, **4**, 1405–1412.
69. Waigmann, E. & Zambryski, P. (1995). Tobacco mosaic virus movement protein-mediated protein transport between trichome cells. *Plant Cell*, **7**, 2069–2079.
70. Canto, T. & Palukaitis, P. (2005). Subcellular distribution of mutant movement proteins of Cucumber mosaic virus fused to green fluorescent proteins. *J. Gen. Virol.* **86**, 1223–1228.
71. Soto, M. J., Chen, L. F., Seo, Y. S. & Gilbertson, R. L. (2005). Identification of regions of the Beet mild curly top virus (family Geminiviridae) capsid protein involved in systemic infection, virion formation and leafhopper transmission. *Virology*, **341**, 257–270.
72. Conti, E., Uy, M., Leighton, L., Blobel, G. & Kuriyan, J. (1998). Crystallographic analysis of the recognition of

a nuclear localization signal by the nuclear import factor karyopherin alpha. *Cell*, **94**, 193–204.
73. Zemanova, L., Schenk, A., Valler, M. J., Nienhaus, G. U. & Heilker, R. (2003). Confocal optics microscopy for biochemical and cellular high-throughput screening. *Drug Discov. Today*, **8**, 1085–1093.
74. Michalet, X., Kapanidis, A. N., Laurence, T., Pinaud, F., Doose, S., Pflughoefft, M. & Weiss, S. (2003). The power and prospects of fluorescence microscopies and spectroscopies. *Annu. Rev. Biophys. Biomol. Struct.* **32**, 161–182.
75. Norrander, J., Kempe, T. & Messing, J. (1983). Construction of improved M13 vectors using oligodeoxynucleotide-directed mutagenesis. *Gene*, **26**, 101–106.
76. Citovsky, V., Knorr, D., Schuster, G. & Zambryski, P. C. (1990). The P30 movement protein of tobacco mosaic virus is a single-strand nucleic acid binding protein. *Cell*, **60**, 637–647.
77. Tzfira, T., Vaidya, M. & Citovsky, V. (2001). VIP1, an *Arabidopsis* protein that interacts with *Agrobacterium* VirE2, is involved in VirE2 nuclear import and *Agrobacterium* infectivity. *EMBO J.* **20**, 3596–3607.
78. Jayaswal, R. K., Veluthambi, K., Gelvin, S. B. & Slightom, J. L. (1987). Double-stranded cleavage of T-DNA and generation of single-stranded T-DNA molecules in *Escherichia coli* by a virD-encoded border-specific endonuclease from *Agrobacterium tumefaciens*. *J. Bacteriol.* **169**, 5035–5045.
79. Tzfira, T., Jensen, C. S., Wangxia, W., Zuker, A., Altman, A. & Vainstein, A. (1997). Transgenic Populus: a step-by-step protocol for its *Agrobacterium*-mediated transformation. *Plant Mol. Biol. Rep.* **15**, 219–235.
80. Kapila, J., De Rycke, R., Van Montagu, M. & Angenon, G. (1997). An *Agrobacterium*-mediated transient gene expression system for intact leaves. *Plant Sci.* **122**, 101–108.
81. Wroblewski, T., Tomczak, A. & Michelmore, R. (2005). Optimization of *Agrobacterium*-mediated transient assays of gene expression in lettuce, tomato and *Arabidopsis*. *Plant Biotech. J.* **3**, 259–273.
82. Draper, J., Scott, R., Armitage, P. & Walden, R. (1988). *Plant Genetic Transformation and Gene Expression, A Laboratory Manual,* Blackwell Scientific Publications Ltd., London.
83. Fromm, M., Taylor, L. P. & Walbot, V. (1985). Expression of genes transferred into monocot and dicot plant cells by electroporation. *Proc. Natl Acad. Sci. USA*, **82**, 5822–5828.

Edited by J. Karn

(Received 20 June 2006; received in revised form 3 August 2006; accepted 3 August 2006)
Available online 11 August 2006